ISSN 1070-3284, Russian Journal of Coordination Chemistry, 2024, Vol. 50, No. 6, pp. 374–383. © Pleiades Publishing, Ltd., 2024.

Crystal Structure of Tetraammine Zinc(II) Peroxodisulfate and Barium Peroxodisulfate Tetrahydrate

A. G. Medvedev[a], T. A. Tripol'skaya[a], E. A. Mel'nik[a], P. A. Egorov[a], N. S. Mayorov[a], A. A. Mikhaylov[a], O. Lev[b, *], and P. V. Prikhodchenko[a, *]

[a] *Kurnakov Institute of General and Inorganic Chemistry, Russian Academy of Sciences, Moscow, Russia*

[b] *The Casali Center of Applied Chemistry, The Institute of Chemistry, The Hebrew University of Jerusalem, Jerusalem, Israel*

**e-mail: prikhman@gmail.com*

Received December 7, 2023; revised January 24, 2024; accepted January 24, 2024

Abstract—Zinc(II) tetraammine peroxodisulfate $[Zn(NH_3)_4]S_2O_8$ (**I**) and barium peroxodisulfate tetrahydrate $BaS_2O_8 \cdot 4H_2O$ (**II**) were synthesized by interaction of an aqueous solution of ammonium peroxodisulfate with a zinc peroxide and barium hydroxide, respectively. The crystal structures (CIF file CCDC nos. 2311248 (**I**) and 2311249 (**II**)) were determined by single crystal X-ray diffraction. The crystal structure of **I**, for which X-ray powder diffraction structural data were previously reported, has been redetermined and clarified. The crystal packing of **I** consists of hydrogen-bonded chains parallel to the *b*-axis connected in a three-dimensional structure with H-bonds between adjacent chains. The compound **II** is coordination polymer with coordination number of barium cation equal to 9. The crystal packing of **II** consists of channels in which water molecules are held by H-bonds. Compounds **I** and **II** were characterized by DTA and TGA revealing thermal stability up to 170 and 90°C.

Keywords: peroxodisulfates, X-ray diffraction, hydrogen bonds, crystal packing

DOI: 10.1134/S1070328423601553

INTRODUCTION

Peroxodisulfates (persulfates) are strong oxidizing agents and sources of radicals, which determine their application in the production of polymers, microelectronics, for etching printed circuit boards, and also as bleaching agents and disinfectants [1]. Persulfates are widely used as oxidants in the organic chemistry [2, 3], for example, for hydroxylation of phenols and arylamines [4], hydrocarboxylation of alkanes [5, 6] and aroylation of electron-rich pyrroles [7]. Despite the importance of persulfate compounds, not many crystal structures have been characterized and most of them contain organic ligands coordinated to the metal cation. Such complex salts were obtained for Ag(II), Fe(III), Zn(II), Cd(II), Mn(III), Mn(IV), Hg(II), Cu(II) and others [8]. However, peroxodisulfates, which contain organic molecules in their structure, are usually unstable or prone to explosive decomposition, which limits their use [9, 10]. The crystal structures of purely inorganic persulfates have been studied much less. An accurate structural characterization based on single-crystal X-ray diffraction analysis has been obtained only for alkali metal and ammonium persulfates, which is likely due to the difficulty of synthesizing pure and single-crystalline samples [11]. At the same time, crystal packing and non-covalent interactions are undoubtedly responsible for the stability of inorganic peroxodisulfates; therefore, the accurate and complete characterization of their crystal structure is an important task.

Previously, the synthesis of tetraammine zinc(II) peroxodisulfate (**I**) was reported and the crystal structure of **I** was described based on its X-ray powder diffraction, which did not allow to obtain enough data for accurate and complete structural characterization [12, 13]. Barium peroxodisulfate hydrates are used as precursors for the preparation of other metal peroxodisulfates by cation exchange reactions with the corresponding sulfates [14]. In this work, we report the crystal structure of **I** as determined by single-crystal X-ray diffraction. The synthesis of **I** was carried out using zinc peroxide powder as a source of zinc(II), which made it possible to obtain good quality single crystals. In addition, the synthesis of barium peroxodisulfate tetrahydrate (**II**) was repeated according to the published procedure [14, 15] and the crystal structure of **II** was determined by SCXRD. Additionally, the thermal stability of **I** and **II** was studied by thermogravimetric and DTA analysis.

EXPERIMENTAL

Materials and methods. Commercial reagents and solvents were used for the synthesis as received:

zinc(II) acetate dihydrate (98%, Sigma Aldrich), hydrogen peroxide (35% aqueous solution, Khimmed), sodium hydroxide (analytical grade, Khimmed), ammonium persulfate (98%, Sigma Aldrich), ammonia (aqueous solution, Khimmed), barium hydroxide octahydrate (special purity grade, Khimmed), ethanol (95%, Acros Organics).

Elemental analysis. Peroxide content was determined by permanganometry [16]. Peroxodisulfate content was determined by iodometry [17]. Zinc content was determined by complexometric titration with EDTA [18]. Barium content was determined by gravimetric analysis as barium sulfate [18].

Differential thermal analysis (DTA) and thermogravimetry analysis (TGA) were conducted using a simultaneous thermal analyzer, DTG-60 (Shimadzu), under argon flow. The experiments were performed in the temperature range of 25–300°C at a heating rate of 10°C/min in aluminum pans. The powders of **I** and **II** were mixed with Al_2O_3 powder (1 : 4 by weight).

Powder X-ray diffraction data of **I** and **II** were collected at room temperature on a Bruker D8 Advance diffractometer using CuK_α radiation (λ = 1.5418 Å) in the range 10° to 60° 2θ with a step size of 0.02° and counting time of 1 s/step. XRD patterns were processed by DiffracPlus software. Theoretical XRD patterns were calculated by Mercury software [19].

Synthesis of ZnO_2. 4.0 g (18.2 mmol) of zinc(II) acetate dihydrate was dissolved in 62 mL of 1 wt % aqueous H_2O_2 (18.2 mmol). 2 wt % NaOH solution was added slowly to the obtained solution to rich the pH of 8.5. The precipitate was separated by centrifugation and washed twice with distilled water, once with ethanol and dried at 75°C for 4 h. The content of zinc peroxide in the resulting powder (estimated by the peroxide content) was 70 wt %.

Synthesis of $[Zn(NH_3)_4]S_2O_8$ (I). Ammonium persulfate $(NH_4)_2S_2O_8$ (0.228 g, 1.0 mmol) was dissolved in 4 mL of concentrated aqueous ammonia. ZnO_2 powder (0.139 g, 1.0 mmol) was dissolved in the ammonium persulfate solution. The resulting solution was placed in the refrigerator at 4°C overnight. The crystalline powder was filtered, washed with 5 mL of cold EtOH and dried. Yield 0.21 g (64.5%).

For $N_4H_{12}O_8S_2Zn$ (**I**)

Anal. calcd, %	Zn, 20.07	$S_2O_8^{2-}$, 59.00
Found, %	Zn, 19.89	$S_2O_8^{2-}$, 60.14

Synthesis of $BaS_2O_8 \cdot 4H_2O$ were performed according to published procedure [12]. Briefly, the solids of $Ba(OH)_2 \cdot 8H_2O$ (1.58 g, 5.0 mmol) and $(NH_4)_2S_2O_8$ (1.14 g, 5.0 mmol) were grinded to form a dispersion. The dispersion was allowed to stand for 15 min and filtered off. The filtrate was evaporated in air in a Petri dish until crystals were formed. Yield 1.59 g (79.3%).

For $H_8S_2O_{12}Ba_1$ (**II**)

Anal. calcd, %	Ba, 34.20	$S_2O_8^{2-}$, 47.85
Found, %	Ba, 33.72	$S_2O_8^{2-}$, 48.61

X-ray crystallography analysis. Single crystal X-ray diffraction study of **I** and **II** was carried out on a Bruker D8 Venture diffractometer (graphite monochromatized MoK_α radiation, λ = 0.71073 Å) using ω-scan mode at 150 and 100 K, respectively. The absorption corrections based on measurements of equivalent reflections were applied [20]. The structure of **I** and **II** were solved by direct method and refined by full matrix least-squares on F^2 with anisotropic thermal parameters for all non-hydrogen atoms [21]. All hydrogen atoms were found from difference Fourier synthesis. Hydrogen atoms in **I** were refined with thermal parameters $U_{iso}(H) = 1.2 \times U_{eq}(N)$ and SADI restraints. O–H distances of water molecules in II were fixed at 0.85 Å. The structure of **I** was refined as a two-component inversion twin with a twin ratio of 0.911(13)/0.089(13). The crystallographic data and structure refinement details for **I** and **II** are summarized in Table 1; selected bond lengths and bond angles are given in Table 2.

The structures of **I** and **II** are deposited with the Cambridge Crystallographic Data Centre (CCDC) (nos. 2311248 and 2311249, respectively; deposit@ccdc.cam.ac.uk or http://www.ccdc.cam.ac.uk/).

Continuous shape measures were performed using the SHAPE v.2.1 program [22].

RESULTS AND DISCUSSION

The procedure for the synthesis of **I** described earlier did not yield single crystals suitable for SCXRD [12]. Previously, the crystal structure of **I** obtained by crystallization from the aqueous solution of ammonium peroxodisulfate and zinc(II) chloride was solved using powder X-ray diffraction as a non-centrosymmetric space group $Pna2_1$ with a $S_2O_8^{2-}$ anion lying on a two-fold axis. The reported crystal structure contains peroxodisulfate anion with O–O distance is 1.465(16) Å. The N–H...O hydrogen bond donor-acceptor distance lying within the range 2.75(2)–2.90(3) Å. However, these distances are shorter than those for compounds containing tetraammine zinc(II) cation (2.9030–3.1810 Å) [8]. In addition, careful analysis of the structure revealed that the peroxodisulfate anion does not lie on the two-fold axis. This indicates that the structure is not correctly solved using powder X-ray diffraction data. In this context, attempts have been made to obtain single crystals suitable for SCXRD.

Table 1. Crystal data and structure refinement for **I** and **II**

Parameter	Value	
	I	**II**
Molecular formula	$H_{12}N_4O_8S_2Zn$	$H_8O_{12}S_2Ba$
M	325.63	401.52
Color, habit	Colorless, prism	Colorless, prism
Cryst size, mm	0.30 × 0.20 × 0.20	0.10 × 0.10 × 0.05
Temperature, K	150	100
System	Orthorhombic	Monoclinic
Space group	$Pna2_1$	$P2_1/c$
a, Å	21.0155(9)	7.4163(3)
b, Å	7.9833(4)	19.5873(8)
c, Å	12.6412(6)	7.4691(3)
α, deg	90	90
β, deg	90	114.336(1)
γ, deg	90	90
V, Å^3	2120.85(17)	988.59(7)
Z	8	4
ρ_{calcd}, g/cm^3	2.040	2.698
$\mu(MoK_\alpha)$, mm^{-1}	2.742	4.495
$F(000)$	1328	768
θ Range, deg	1.94 to 28.99	2.08 to 28.00
Total number of reflections	30443	13891
Number of unique reflections (R_{int})	5636 (0.057)	2382 (0.023)
Number of reflections $I > 2\sigma(I)$	5054	2237
Number of refined parameters	339	168
R_1 ($I > 2\sigma(I)$)	0.0280	0.0128
wR_2 (all data)	0.0648	0.0307
GOOF	1.036	1.083
$\Delta\rho_{min}$ /$\Delta\rho_{max}$, e/Å^3	−0.41/0.47	−0.57/0.43

Previously, it has been shown that metal peroxides can be used as starting compounds in inorganic synthesis. For example, barium peroxide was used for the hydrothermal synthesis of $NaBa[Rh(OH)_6]$ [23]. We used zinc peroxide to synthesize compound **I**, which allowed us to grow large crystals suitable for SCXRD.

The colourless crystals of $[Zn(NH_3)_4]S_2O_8$ (**I**) were grown by cooling a solution obtained by dissolving zinc peroxide and ammonium persulfate in aqueous ammonia. Zinc peroxide nanoparticles have previously been reported as a source of hydrogen peroxide [24] and a precursor for zinc oxide and sulfide coatings [25–29]. Compound **I** crystallizes in the $Pna2_1$ space group according to the SCXRD experiment performed at 150 K (Table 1), in agreement with previously published data obtained at room temperature. The cell parameters are different, resulting in about twice the cell volume (Table 1). The asymmetric unit of **I** is represented by two $[Zn(NH_3)_4]^{2+}$ cations with the tetrahedral environment of Zn(II) and two $S_2O_8^{2-}$ anions (Fig. 1).

The CSD includes only 5 entries of peroxodisulfate-containing zinc(II) complexes, in all of which Zn(II) serves as the hexacoordinated metal centre and in two cases the peroxodisulfate acts as a ligand. The Zn–N bond lengths vary in the range 1.997(5)–2.034(4) Å (Table 2), which is comparable to the values reported in CSD [8] and slightly shorter than for the reported crystal structure of $[Zn(NH_3)_4]S_2O_8$ [12]. A slightly distorted tetrahedral geometry is indicated by NZnN angles in the range 104.6(2)°–115.6(2)°. The glide plane passes through the midpoint of O–O bonds of peroxodisulfate anions. The O–O bond

Table 2. Selected bond lengths (Å) and angles (deg) for **I** and **II***

Bond	*d*, Å	Bond	*d*, Å
	I		
Zn(1)–N	2.006(4)–2.034(4)	Zn(2)–N	1.997(5)–2.019(4)
S(1)–O_t	1.438(3)–1.449(4)	S(3)–O_t	1.420(5)–1.445(3)
S(1)–O(4)	1.653(3)	S(3)–O(12)	1.646(3)
S(2)–O_t	1.435(3)–1.437(3)	S(4)–O_t	1.428(3)
S(2)–O(5)	1.663(3)	S(4)–O(13)	1.674(3)
O(4)–O(5)	1.476(4)	O(12)–O(13)	1.482(4)
	II		
Ba(1)–O	2.769(1)–2.883(1)	S(2)–O_t	1.438(1)–1.441(1)
S(1)–O_t	1.434(1)–1.448(1)	S(2)–O(4)	1.661(1)
S(1)–O(5)	1.644(1)	O(4)–O(5)	1.476(2)
Angle	ω, deg	Angle	ω, deg
	I		
NZn(1)N	104.6(2)–115.6(2)	NZn(2)N	105.2(2)–114.9(2)
O_tS(1)O_t	114.2(2)–115.6(2)	O_tS(2)O_t	114.3(2)–116.0(2)
O_tS(1)O(4)	97.9(2)–106.5(2)	O_tS(2)O(5)	96.6(2)–106.2(2)
O_tS(3)O_t	113.8(2)–115.7(2)	O_tS(4)O_t	114.1(2)–116.0(2)
O_tS(3)O(12)	97.5(2)–107.4(2)	O_tS(4)O(13)	96.4(2)–106.3(2)
S(1)O(4)O(5)S(2)	–129.2(2)	S(3)O(12)O(13)S(4)	–130.3(2)
	II		
O_tS(1)O_t	114.2(1)–115.7(1)	O_tS(2)O(4)	98.2(1)–106.8(1)
O_tS(1)O(5)	96.9(1)–107.0(1)	S(2)O(4)O(5)S(1)	124.4(1)
O_tS(2)O_t	114.0(1)–115.3(1)		

lengths in the anions are 1.476(4) and 1.482(4) Å, in agreement with reported values [8, 11]. The S–O distance values are presented in Table 2.

The crystal structure of **I** is stabilized by a rich network of N–H...O hydrogen bonds involving ammine ligands with peroxodisulfate anions (Table 3). The donor-acceptor distances vary in the range of 2.984(5)–3.187(5) Å. The hydrogen bonds bind adjacent cations and anions in a chains parallel to the *b* axis (Fig. 2), which form 3D structure due to H-bonds between neighboring chains (Fig. 3). Thus, crystal **I** is the first inorganic peroxodisulfate containing a Zn(II) with a tetrahedral environment.

Barium peroxide did not react with an aqueous solution of ammonium peroxodisulfate, apparently due to the low solubility of BaO_2. Therefore, the colorless crystals of $BaS_2O_8{\cdot}4H_2O$ (**II**) were grown from a dispersion obtained by grinding of barium hydroxide and ammonium persulfate. Compound **II** crystallizes in the $P2_1/c$ space group (Table 1). The asymmetric unit of **II** includes one Ba^{2+} cation, one persulfate anion, and four water molecules (Fig. 4). The Ba(1) cation environment comprises nine oxygen atoms, with six being part of five peroxodisulfate anions, while the remaining three are associated with water molecules (Fig. 5). The {BaO_9} coordination polyhedron can be classified as a spherical capped square antiprism (CSAPR-9, *C*4*v*) or a Muffin shape (MFF_9, C_s) by means of continuous shape measures [22, 30]. Two adjacent {BaO_9} polyhedral share an edge whose vertices are occupied by oxygen atoms O(9) of the water molecules (Fig. 5). One anion is coordinated by two oxygen atoms (O(3) and O(8)) for each Ba cation. The O–O distance value of anion equal to 1.476(2) Å which is in agreement with crystal **I** and other persulfates. The anion geometry closely resembles that found in **I** (see Table 2).

A barium cation, persulfate anion, two coordinated water molecules, and two solvated molecules together form a three-dimensional structure, further stabilized with moderate O–H...O hydrogen bonds (Fig. 6, Table 4). All hydrogen atoms participate in the formation of hydrogen bonds. It should be noted, the oxygen atom O(11) acts only as acceptor of hydrogen bonds, and do not form hydrogen bonds as proton donor. The second solvate water molecule (H(12A)–O(12)–

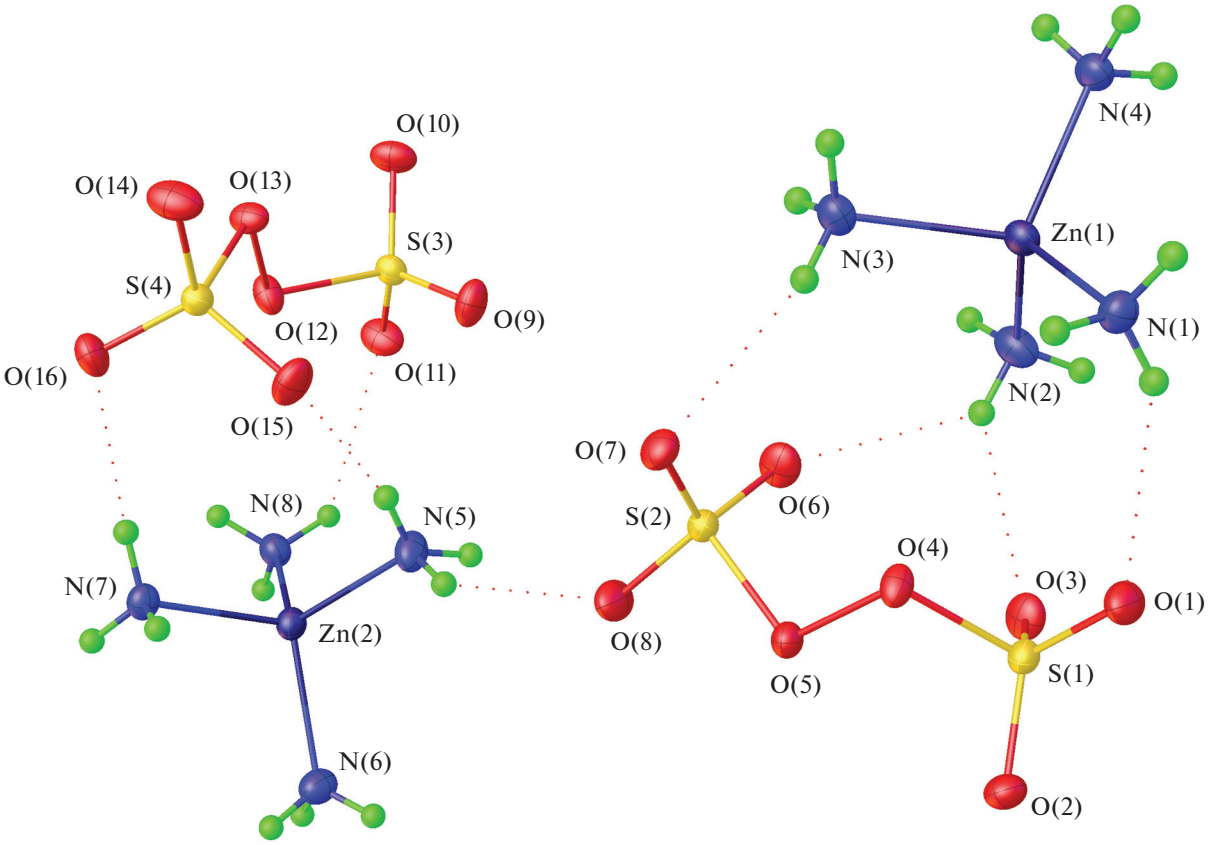

Fig. 1. Asymmetric unit in **I**. Thermal ellipsoids are drawn at 50% probability level. H-bonds are shown by dashed lines.

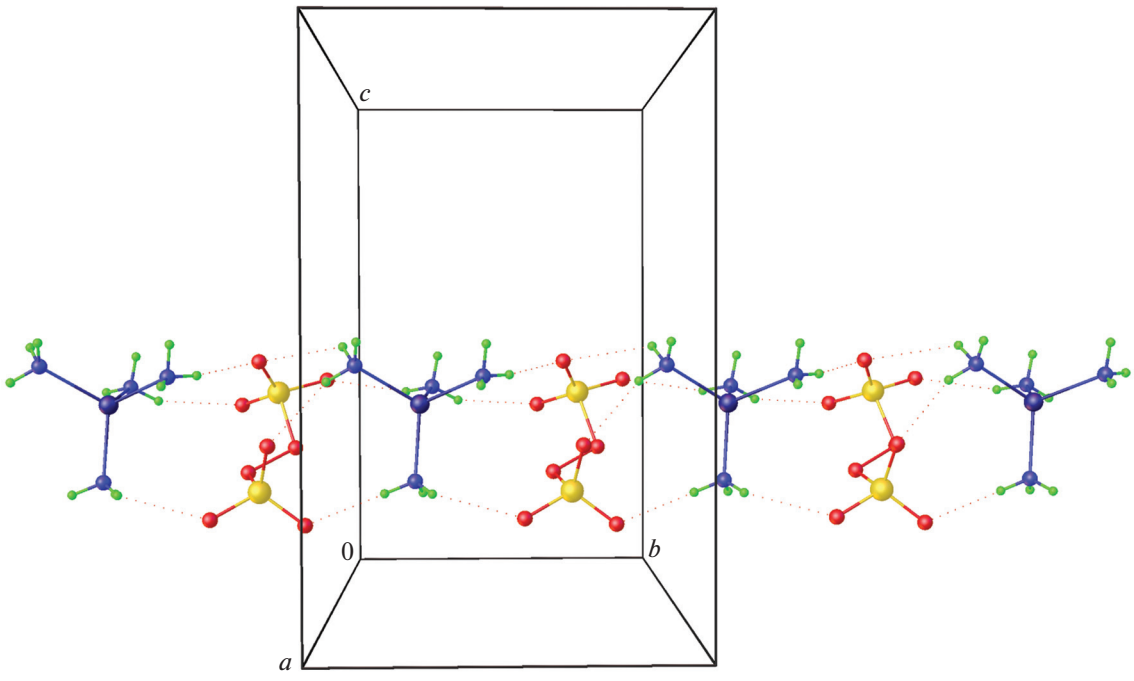

Fig. 2. Hydrogen bonded chains parallel to *b* axis in **I**. H-bonds are shown by dashed lines.

Table 3. Geometric parameters of hydrogen bonds for **I***

Contact *D*–H···*A*	Distance, Å			Angle DHA, deg
	D–H	H···*A*	*D*···*A*	
N(1)–H(1C)···O(2)^{i}	0.80(3)	2.28(3)	3.060(5)	168(5)
N(1)–H(1B)···O(1)	0.80(3)	2.33(4)	3.026(5)	147(5)
N(1)–H(1A)···O(16)^{ii}	0.82(3)	2.32(3)	3.122(5)	165(5)
N(2)–H(2A)···O(3)	0.82(3)	2.31(4)	3.039(6)	149(5)
N(2)–H(2C)···O(10)^{iii}	0.79(3)	2.50(3)	3.260(5)	160(5)
N(3)–H(3A)···O(1)^{iv}	0.86(3)	2.26(3)	3.089(5)	163(4)
N(3)–H(3B)···O(7)	0.87(3)	2.32(3)	3.101(5)	150(4)
N(3)–H(3C)···O(8)	0.88(3)	2.21(3)	3.040(5)	157(5)
N(4)–H(4A)···O(3)^{i}	0.87(3)	2.23(3)	3.028(6)	153(4)
N(4)–H(4B)···O(2)^{iv}	0.85(3)	2.32(4)	3.079(5)	148(4)
N(4)–H(4C)···O(11)^{iii}	0.87(3)	2.40(4)	3.109(5)	139(4)
N(4)–H(4C)···O(14)^{v}	0.87(3)	2.37(4)	2.992(5)	129(4)
N(5)–H(5A)···O(8)	0.89(3)	2.29(4)	2.984(5)	135(4)
N(5)–H(5B)···O(2)^{vi}	0.85(3)	2.47(3)	3.187(5)	142(4)
N(5)–H(5C)···O(15)	0.89(3)	2.15(3)	3.003(5)	160(4)
N(6)–H(6A)···O(15)^{vii}	0.82(3)	2.36(3)	3.154(5)	166(4)
N(6)–H(6C)···O(1)^{vi}	0.83(3)	2.43(4)	3.151(5)	146(4)
N(7)–H(7A)···O(10)^{viii}	0.83(3)	2.27(3)	3.067(5)	162(5)
N(7)–H(7B)···O(16)	0.83(3)	2.36(3)	3.114(5)	152(5)
N(7)–H(7C)···O(14)^{vii}	0.84(3)	2.22(3)	2.988(5)	153(5)
N(8)–H(8A)···O(10)^{vii}	0.84(3)	2.19(3)	3.031(5)	179(5)
N(8)–H(8B)···O(7)^{ix}	0.84(3)	2.28(3)	3.097(5)	162(6)
N(8)–H(8C)···O(3)^{vi}	0.82(3)	2.56(4)	3.155(5)	130(4)
N(8)–H(8C)···O(11)	0.82(3)	2.44(3)	3.072(5)	135(3)

* Symmetry codes: (i) $x, y + 1, z$; (ii) $-x + 1/2, y + 1/2, z + 1/2$; (iii) $-x + 1, -y + 2, z + 1/2$; (iv) $-x + 1, -y + 2, z - 1/2$; (v) $x + 1/2, -y + 5/2, z$; (vi) $-x + 1, -y + 1, z - 1/2$; (vii) $x, y - 1, z$; (viii) $-x + 1/2, y - 1/2, z + 1/2$; (ix) $-x + 1/2, y - 1/2, z - 1/2$.

H(12B)) participates in the formation of two hydrogen bonds as a proton donor and two as a proton acceptor and is located in the channels parallel to *a* axis (Fig. 6).

The phase purity of powders **I** and **II** was confirmed by X-ray powder diffraction revealing no crystalline impurities (Fig. 7).

The thermal stability of **I** was evaluated with a mixture of Al_2O_3 powder, considering the significant thermal effect of decomposition. Compound **I** demonstrates high thermal stability and begins to decompose exothermically at 172°C with a peak at 185°C. This is notably higher than that of initial ammonium persulfate, which has a decomposition temperature of 120°C [31]. Compound **II** releases water with endothermic effect with maximum at 60°C, followed by exothermic decomposition of persulfate with onset at 85°C and peak at 95°C.

ACKNOWLEDGMENTS

X-ray diffraction studies were performed at the Centre of Shared Equipment of Kurnakov Institute of General and Inorganic Chemistry, Russian Academy of Sciences.

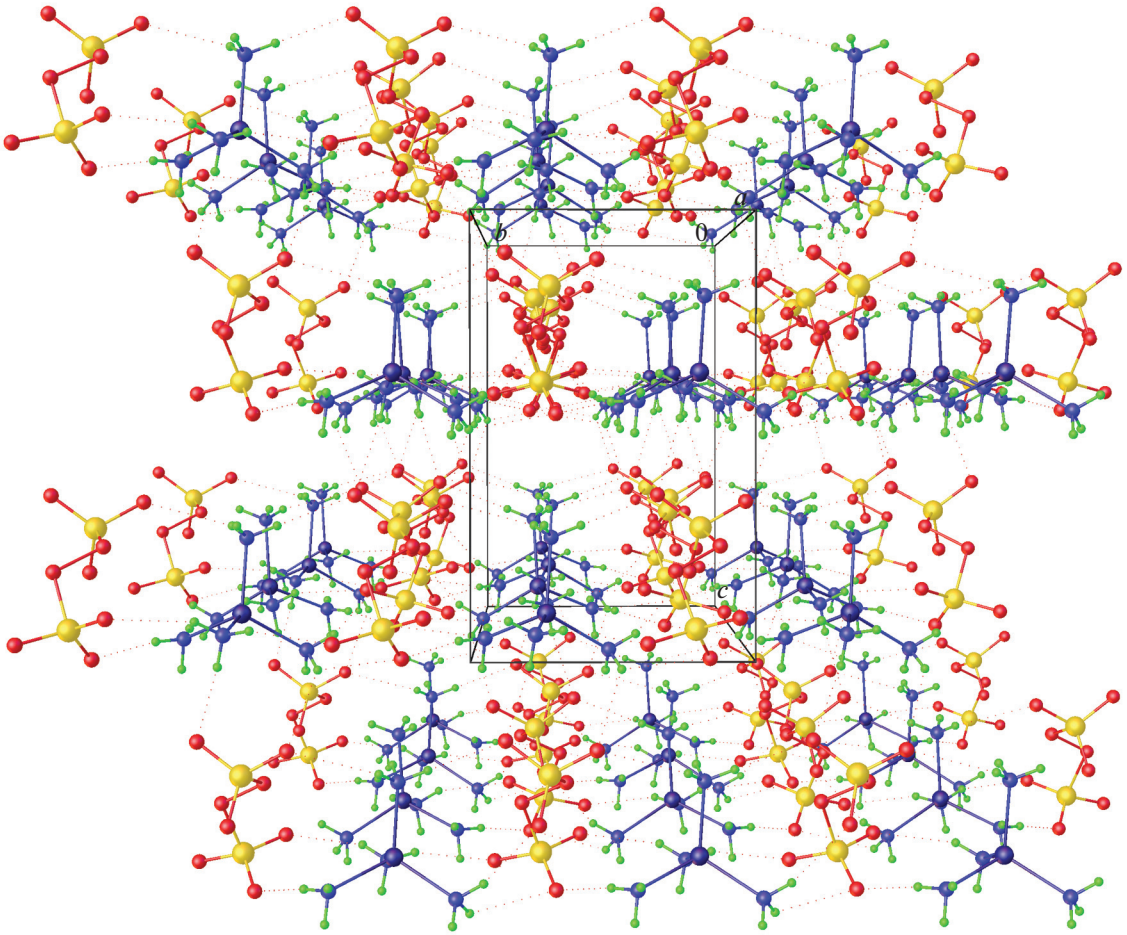

Fig. 3. Crystal packing in **I**. H-bonds are shown by dashed lines.

Table 4. Geometric parameters of hydrogen bonds for **II***

Contact *D*–H···*A*	Distance, Å			Angle DHA, deg
	D–H	H···*A*	*D*···*A*	
O(9)–H(9B)···O(12)	0.86(2)	1.95(2)	2.782(2)	162(3)
O(9)–H(9A)···O(12)^{i}	0.83(2)	2.00(2)	2.807(2)	163(2)
O(10)–H(10B)···O(11)	0.85(2)	1.94(2)	2.776(2)	171(3)
O(10)–H(10A)···O(11)^{ii}	0.84(2)	2.00(2)	2.807(2)	163(3)
O(12)–H(12A)···O(7)	0.84(2)	2.03(2)	2.863(2)	172(3)
O(12)–H(12B)···O(10)^{iii}	0.82(2)	2.09(2)	2.866(2)	157(3)

* Symmetry codes: (i) $-x, -y + 1, -z + 1$; (ii) $x, -y + 1/2, z + 1/2$; (iii) $-x + 1, -y + 1, -z + 1$.

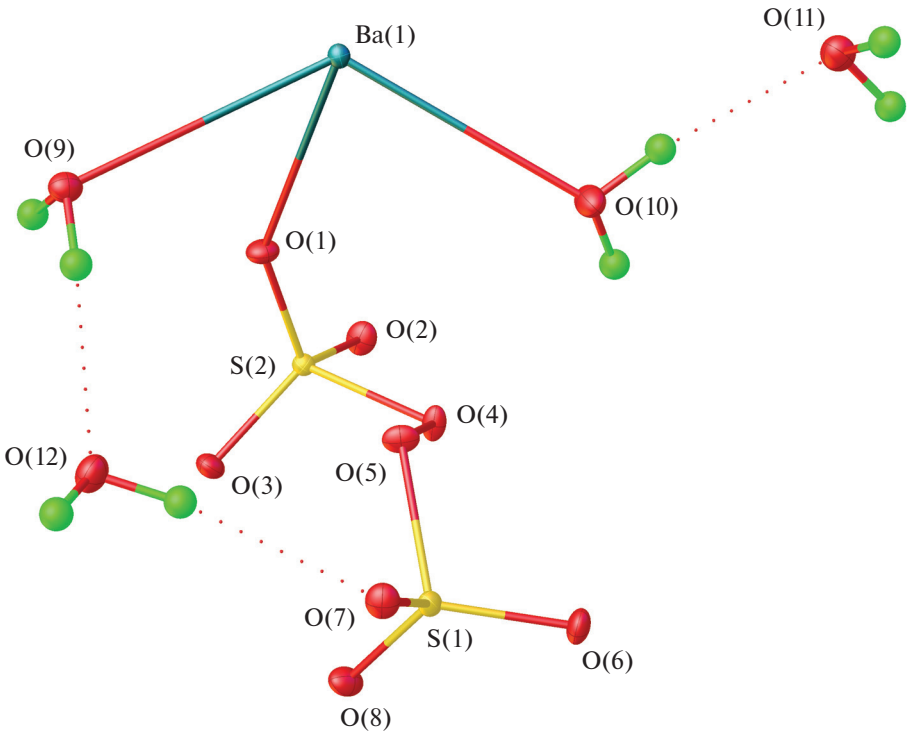

Fig. 4. Asymmetric unit in **II**. Thermal ellipsoids are drawn at 50% probability level. H-bonds are shown by dashed lines.

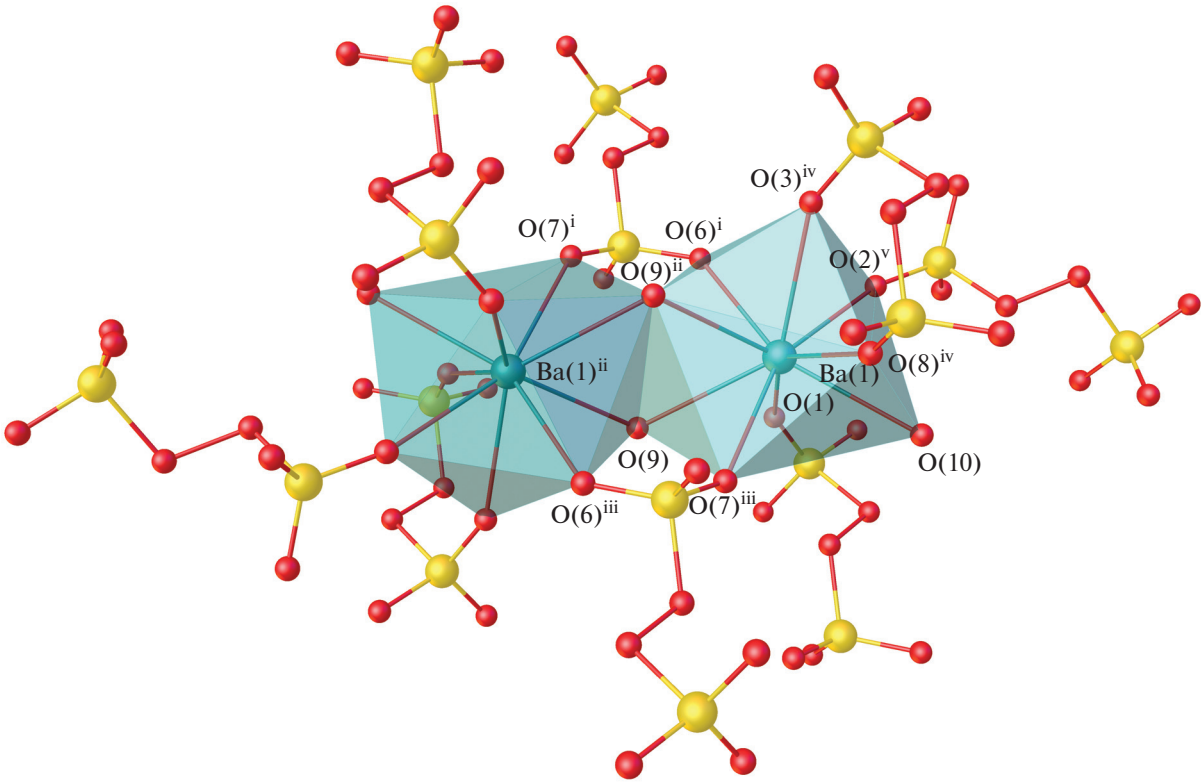

Fig. 5. Fragment of the crystal structure of **II**. Symmetry codes: (i) $x-1, y, z-1$; (ii) $-x, 1-y, -z$; (iii) $1-x, 1-y, 1-z$; (iv) $x, y, z-1$; (v) $x, 1/2-y, -1/2+z$.

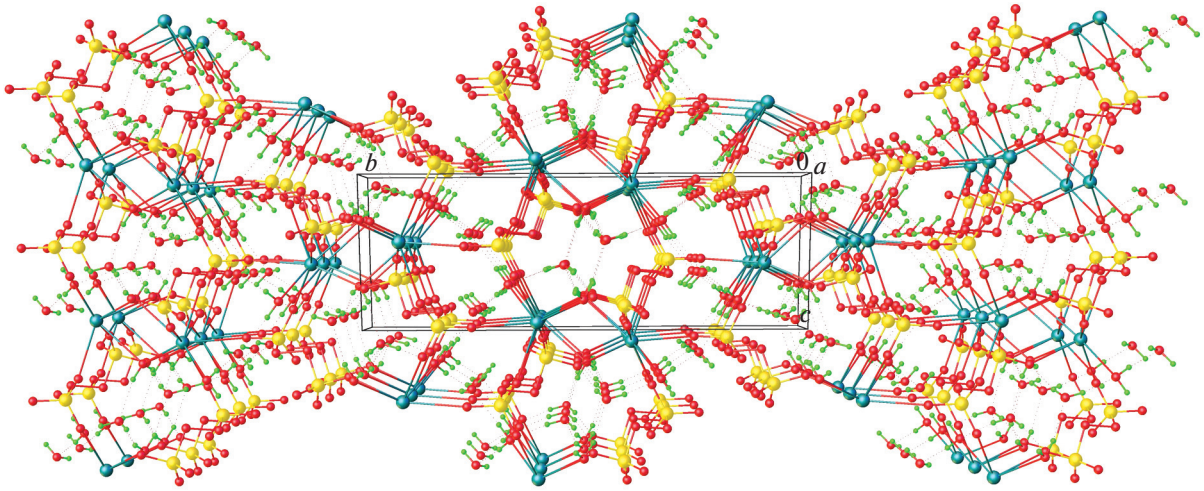

Fig. 6. Crystal packing in **II**. H-bonds are shown by dashed lines.

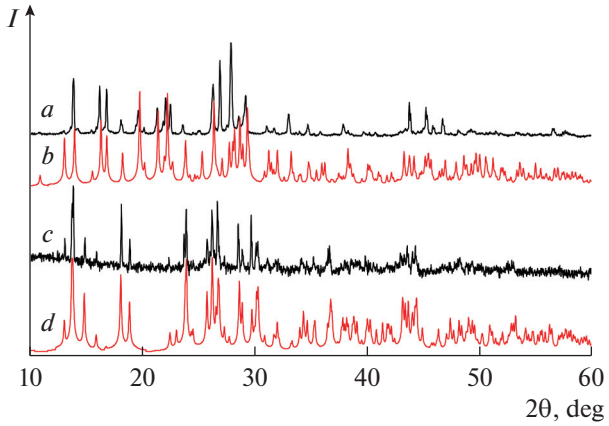

Fig. 7. Powder X-ray diffractograms of $[Zn(NH_3)_4]S_2O_8$ (**I**, *a*) and $BaS_2O_8 \cdot 4H_2O$ (**II**, *c*) and their calculated diffractograms (*b* and *d*, respectively).

FUNDING

This study was supported by the Russian Science Foundation (grant no. 23-23-00596; https://rscf.ru/en/project/23-23-00596/).

CONFLICT OF INTEREST

The authors of this work declare that they have no conflicts of interest.

REFERENCES

1. Jakob, H., Leininger, S., Lehmann, T., et al., *Ullmann's Encyclopedia of Industrial Chemistry*, Wiley, 2000. https://doi.org/10.1002/14356007.a19_177.pub2
2. Jones, C.W., *Applications of Hydrogen Peroxide and Derivatives*, Cambridge: Royal Society of Chemistry, 1999. https://doi.org/10.1039/9781847550132
3. Ma, Z., Mahmudov, K.T., Aliyeva, V.A., et al., *Coord. Chem. Rev.*, 2021, vol. 437, p. 213859. https://doi.org/10.1016/j.ccr.2021.213859
4. Behrman, E.J., *Organic Reactions*, Wiley, 1988, p. 421. https://doi.org/10.1002/0471264180.or035.02
5. Kirillova, M.V., Kirillov, A.M., Martins, A.N.C., et al., *Inorg. Chem.*, 2012, vol. 51, no. 9, p. 5224. https://doi.org/10.1021/ic300123d
6. Kirillov, A.M., Karabach, Y.Y., Kirillova, M.V., et al., *Cryst. Growth Des.*, 2012, vol. 12, no. 3, p. 1069. https://doi.org/10.1021/cg201459k
7. Kumar, S. and Padala, K., *Chem. Commun.*, 2020, vol. 56, no. 96, p. 15101. https://doi.org/10.1039/D0CC06036D
8. Groom, C.R., Bruno, I.J., Lightfoot, M.P., et al., *Acta Crystallogr., Sect. B: Struct. Sci.*, 2016, vol. 72, no. 2, p. 171. https://doi.org/10.1107/S2052520616003954
9. Guo, Y.-F., Mahmood, S., Xu, B.-H., et al., *J. Org. Chem.*, 2017, vol. 82, no. 3, p. 1591. https://doi.org/10.1021/acs.joc.6b02775
10. Manson, J.L., Stone, K.H., Southerland, H.I., et al., *J. Am. Chem. Soc.*, 2009, vol. 131, no. 13, p. 4590. https://doi.org/10.1021/ja9005223
11. Hellenbrandt, M., *Crystallogr. Rev.*, 2004, vol. 10, no. 1, p. 17. https://doi.org/10.1080/08893110410001664882
12. Skogareva, L.S., Minaeva, N.A., and Filippova, T.V., *Russ. J. Inorg. Chem.*, 2009, vol. 54, no. 9, p. 1341. https://doi.org/10.1134/S0036023609090010
13. Barbieri, G.A. and Calzolari, F., *Z. Anorg. Chem.*, 1911, vol. 71, no. 1, p. 347. https://doi.org/10.1002/zaac.19110710132
14. Marshall, H., *J. Chem. Soc., Trans.*, 1891, vol. 59, p. 771. https://doi.org/10.1039/CT8915900771
15. Ippolitov, E.G., Skogareva, L.S., and Filippova, T.V., *Russ. J. Inorg. Chem.*, 1998, vol. 43, no. 1, p. 5.

16. Schumb, W.C., Satterfield, C.N., and Wentworth, R.L., *Hydrogen Peroxide*, Reinhold, 1955. https://doi.org/10.1002/jps.3030450224
17. Wahba, N., El Asmar, M.F., and El Sadr, M.M., *Anal. Chem.*, 1959, vol. 31, no. 11, p. 1870. https://doi.org/10.1021/ac60155a059
18. Charlot, G., *Les Methodes de La Chimie Analytique: Analyse Quantitative Minérale*, Masson, 1966.
19. Macrae, C.F., Sovago, I., Cottrell, S.J., et al., *J. Appl. Crystallogr.*, 2020, vol. 53, no. 1, p. 226. https://doi.org/10.1107/S1600576719014092
20. Sheldrick, G.M. *SADABS ver. 2016/2,* Bruker AXS, 2016.
21. Sheldrick, G.M., *Acta Crystallogr., Sect. C: Struct. Chem.*, 2015, vol. 71, p. 3. https://doi.org/10.1107/S2053229614024218
22. Llunell, M., Casanova, D., Cirera, J., et al., *SHAPE. Program for the Stereochemical Analysis of Molecular Fragments by Means of Continuous Shape Measures and Associated Tools*, Barcelona: Universitat de Barcelona, 2013.
23. Cook, D.S., Clarkson, G.J., Dawson, D.M., et al., *Inorg. Chem.*, 2018, vol. 57, no. 17, p. 11217. https://doi.org/10.1021/acs.inorgchem.8b01797
24. Wolanov, Y., Prikhodchenko, P.V., Medvedev, A.G., et al., *Environ. Sci. Technol.*, 2013, vol. 47, no. 15, p. 8769. https://doi.org/10.1021/es4020629
25. Shames, A.I., Lev, O., Mikhaylov, A.A., et al., *J. Phys. Chem., C*, 2019, vol. 123, no. 34, p. 20884. https://doi.org/10.1021/acs.jpcc.9b04523
26. Mikhaylov, A.A., Medvedev, A.G., Buldashov, I.A., et al., *J. Alloys Compd.*, 2022, vol. 910, p. 164769. https://doi.org/10.1016/j.jallcom.2022.164769
27. Mikhaylov, A.A., Medvedev, A.G., Grishanov, D.A., et al., *Adv. Mater. Interfaces*, 2019, vol. 6, no. 12, p. 1900368. https://doi.org/10.1002/admi.201900368
28. Uekawa, N., Mochizuki, N., Kajiwara, J., et al., *Phys. Chem. Chem. Phys.*, 2003, vol. 5, no. 5, p. 929. https://doi.org/10.1039/b210990e
29. Raha, S. and Ahmaruzzaman, M., *Nanoscale Adv.*, 2022, vol. 4, no. 8, p. 1868. https://doi.org/10.1039/D1NA00880C
30. Ruiz-Martínez, A., Casanova, D., and Alvarez, S., *Chem. Eur. J.*, 2008, vol. 14, no. 4, p. 1291. https://doi.org/10.1002/chem.200701137
31. Abdel-Kader, M.M., Mosaad, M.M., and El-Kabbany, F.A., *Phys. Status Solidi*, 1992, vol. 130, no. 2, p. 351. https://doi.org/10.1002/pssa.2211300211